Simulated gold clusters and relative extended x-ray-absorption fine-structure spectra

Gregorio D'Agostino
Ente per le Nuove Tecnologie l' Energia e l' Ambiente, Centro Ricerche Energetiche della Casaccia, Progetto Materiali Metallici Innovativi, Casella Postale 2400, I-00100 Roma, Italy

Angelo Pinto
Dipartimento di Fisica, Universitá di Catania, Consorzio Interuniversitario Fisica della Materia, Corso Italia 57, 95129 Catania, Italy and Laboratori Nazionali di Frascati dell'Instituto Nazionale di Fisica Nucleare, 00044 Frascati, Italy

Settimio Mobilio
Dipartimento di Energetica, Universitá de L'Aquila, Roio Monteluco, 67100 L'Aquila and Laboratori Nazionali di Frascati dell'Instituto Nazionale di Fisica Nucleare, 00044 Frascati, Italy
(Received 2 March 1993; revised manuscript received 13 August 1993)

Using a tight-binding many-body potential we estimated classical ground states for gold clusters of various structures and sizes. Cluster contractions are observed as expected. We obtained cluster vibrational properties at very low temperature by evaluating phonon spectra in the pure harmonic approximation. Finally we simulated extended x-ray-absorption fine structure for both the icosahedral and the fcc structures. At sizes corresponding to the closed shells in the icosahedral and cuboctahedral packages, the icosahedral clusters turn out to be more cohesive than the corresponding fcc ones. Critical comparison with available experimental data suggests the presence of such structures in samples obtained by evaporation.

INTRODUCTION

The determination of the structure of very small crystals is a very hard problem to deal with, due to difficulties in sample preparation and to the failure of all structural experimental techniques in studying such systems.

The most serious problem arising in cluster preparation is the uncertainty concerning the size of the clusters, whose dimensions have generally a rather wide distribution. This size dispersion makes difficult the interpretation of any kind of experimental data.

At small cluster dimensions, theoretical calculations foresee for fcc metals a structural change from the parent crystal structure to an icosahedral one. However, up to now no clean evidence of such a structural transition exists. As a matter of fact, due to the large surface to volume ratio present in small clusters, a large relaxation of the atomic positions occurs with respect to the atomic positions of an ideal structure. Such relaxation determines a large amount of static disorder that hinders the differences between different structures.

Recently, some authors[1] employed the Schmid process[2] to obtain monodisperse gold clusters containing 55 atoms. By using extended x-ray-absorption fine-structure (EXAFS) techniques they found the structure to be consistent with fcc cuboctahedral. Also other authors reached the same conclusion on the structure of supported metal cluster using EXAFS techniques applied to polydisperse samples. Balerna *et al.*[3] argued that no icosahedral structure was actually present for Au clusters down to 15 Å in diameter. The same was claimed, for Cu clusters, by Montano *et al.*[4] whose data were consistent with a fcc structure. The previous authors rejected the icosahedral structural hypothesis because: (1) they have not observed a splitting of the first peak in the radial distribution, as predicted by Farges *et al.*,[5] and (2) the dispersion of first-neighbor distances obtained from the structural disorder factors were smaller than the theoretical ones foreseen for the icosahedral shapes.

However, such conclusions cannot be considered definite. In fact, as already outlined,[6] the peak split arises only for polycosahedra and not for Mackay giant icosahedra.[7] Moreover for such a structure the dispersion in first-neighbor distances does not increase drastically.

EXAFS is a very powerful structural technique but it measures mean values of interatomic distances, coordination numbers, and static disorder. Therefore the abovementioned small cluster relaxation makes any interpretation of the structure not definitive when based of EXAFS data only. In this contest, theoretical calculations such as Monte Carlo (MC) and molecular-dynamics (MD) simulations may be of paramount importance both in the interpretation of the experimental data and in assessing the sensitivity of an experimental technique to discern between different structures.

Aimed at this purpose, we performed MD quenching simulations for determining the structure of gold clusters containing from 55 up to 1000 atoms. We then evaluated the phonon spectra for the icosahedral-like and the cuboctahedral-like structures. EXAFS for the former structures were finally simulated.

MODEL AND COMPUTATIONS

All numerical computations were performed using a quasiempirical potential in the tight-binding model (see

Ref. 9 and references therein). It consists of a repulsive Born-Mayer potential and a many-body attractive term that results from the hypothesis of exponential radial behavior of hopping integrals. This leads to the following analytic form:

$$V=\sum_{i=1}^{N}(\Phi_i-\sqrt{\psi_i}) , \tag{1}$$

where

$$\Phi_i=\sum_{j=1}^{N} A \exp\left[-p\frac{r_{ij}}{r_0}\right] , \tag{2}$$

$$\psi_i=\sum_{j=1}^{N} \xi^2 \exp\left[-2q\frac{r_{ij}}{r_0}\right] . \tag{3}$$

The r_{ij} are the atoms distances, r_0 is the first-neighbor distance on the stable gold lattice at $T=0$ K, and A, ξ, p, and q are empiric parameters that characterize the element to be simulated. The square root in formula (1) determines the many-body character of the attractive (Ψ) part of the potential. As Finnis and Sinclair[8] pointed out, the same potential expression may arise in the embedded-atom method (EAM) scenario.

For the empiric constants A, ξ, p, and q we have fixed values previously obtained for the Au metal by fitting the bulk modulus, the elastic constants C_{12}, and C_{44}, stability conditions and the cohesion energy extrapolated at $T=0$ K.[10]

This was performed by evaluating analytically the various constants (C_{11}, C_{12}, etc.) as function of the free parameters and minimizing their difference from the experimental values. A fifth-neighbor cutoff (6.7 Å) in the potential turned out to be adequate to reproduce gold bulk properties in a wide range of temperatures.[10] The values of the parameters resulting from the best fit are reported in Table I.

The same kind of potential has been successfully applied to other systems such as nickel[11] and copper,[12] reproducing correctly elastic and structural properties in a wide range of temperatures even in the presence of very extended defects. These fruitful results encouraged us to extend the application of this kind of potential to clusters.

Recently, some authors[13] developed a more appropriate method for evaluating potential energy for metal clusters, taking into account finite-size effects and electron-shell contributions to cohesion energy. Unfortunately, the former method does not lead to an analytical expression of the energy vs the atomic positions and then it is not practical for MD simulations.

A many-body potential was previously applied to clusters, by Marville and Andreoni,[14] that used a Finnis-Sinclair potential for simulating the structural properties of various transition-metal clusters. More recently Ercolessi, Andreoni, and Tosatti[15] have studied gold cluster melting.

TABLE I. Potential parameters resulting from optimization.

A (eV)	ξ (eV)	p	q
0.2061	1.790	10.229	4.036

Following van de Waals[16] and Boyer and Broughton,[17] in order to obtain minimal energy configurations we considered three fundamental structures: icosahedral, cuboctahedral, and troncoctahedral (or Wulff polyhedron). We started from such configurations and then quenched the systems with the Beeler and Kulcinsky method.[18] We reached different minima for each initial configuration. Table II reports energy per particle for each cuboctahedral, icosahedral, and troncoctahedral relaxed configuration obtained.

Our results on cohesive energies agree with the values obtained with a Sutton-Chen potential by Uppenbrink and Wales[6] up to 1%. The agreement improves with increasing cluster size.

All values referred to a fixed structure were then used to perform nuclear fits, i.e., to fit the following formula:

$$\frac{E}{N}=V_0+aN^{-1/3}+bN^{-2/3} , \tag{4}$$

where the constants V_0, a, and b represent, respectively, the volume, surface, and curvature specific energies. Numerical values resulting from fits are reported in Table III.

As it can be seen looking at Fig. 1, the troncoctahedron is the most cohesive structure apart from $N=13$ system for which the icosahedral structure is preferred. This implies that, as far as it is possible, the system tends to assume fcc troncoctahedral structures. Since one cannot build up troncoctahedral clusters of any size, away from closed troncoctahedral shells, the cuboctahedron becomes more representative of the fcc structures. In these cases icosahedral clusters result to be more cohesive than the fcc ones of the same size. Then one expects icosahedral structure to appear. Up to now there has been no experimental evidence that the icosahedral shape is the favorite one for clusters of any selected size.

Comparison with EXAFS data

EXAFS permit one to obtain a great amount of structural information. The most accurate one is the mean first-neighbor distance,[19] that is related to the leading frequency of the experimental signal. In Fig. 2(a) we

TABLE II. Energy per particle for cuboctahedral, icosahedral, and troncoctahedral relaxed configurations.

N	$E_{\rm cub}/N$ (eV)	$E_{\rm ico}/N$ (eV)	$E_{\rm tr}/N$ (eV)
13	−3.240	−3.273	
38			−3.432
55	−3.463	−3.468	
147	−3.543	−3.555	
201			−3.586
309	−3.599	−3.603	
561	−3.632	−3.634	
586			−3.645
923	−3.655	−3.655	
1289			−3.676
1415	−3.670	−3.671	

TABLE III. Nuclear fit parameters for the three different structures into account.

	V_0 (eV)	a (eV)	b (eV)
Icosahedral	−3.7707	1.1148	0.1290
Cuboctahedral	−3.7798	1.2063	0.1511
Troncoctahedral	−3.7789	1.0868	0.2599

compare the average first-neighbor distances obtained for each quenched configuration, with the experimental values of Ref. 3. The icosahedral curves lie at the top of the graphics while the troncoctahedral and the cuboctahedral ones follow it. All the structures turn out to be contracted with respect to the lattice parameter of the bulk ($r_1 = 2.88$ Å). The comparison with the experimental data suggest that (1) for cluster diameters larger than 40 Å the leading structures are fcc ones; (2) experimental points near troncoctahedral configurations ($d = 20$ Å and $d = 30$ Å) are compatible with such a structure; (3) far away from troncoctahedral configurations ($d = 15$ Å and $d = 24$ Å) the mean first-neighbor distance is not compatible with a cuboctahedron structure while fitting the icosahedral one.

All the previous qualitative observations are in close agreement with the theoretical predictions on cluster stability. Moreover it must be emphasized that our computations do not actually predict the presence of only one structure. In fact, in macroscopic samples several structures may coexist with relative frequencies depending on their free energies. At this respect some authors[20] observed time fluctuation between different gold cluster structures. For the sake of completeness we reported in Fig. 2(b) theoretical and experimental data relative to the second shell. In this case the presence of significant error bars does not allow to gain any information.

Other relevant quantities measurable by EXAFS are the first- and second-neighbor coordinates. Figure 3

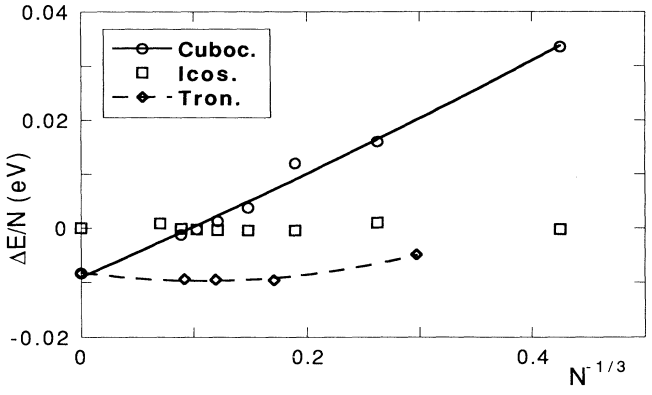

FIG. 1. Energy per particle vs cluster size for different structures. We subtracted the icosahedral fitted energies to all curves in order to enhance their very slight differences. For actual values one may refer to Table I in the text. The labels Cuboc., Icos., and Tronc. refer, respectively, to the cuboctahedral, icosahedral, and troncoctahedral closed-shell structures.

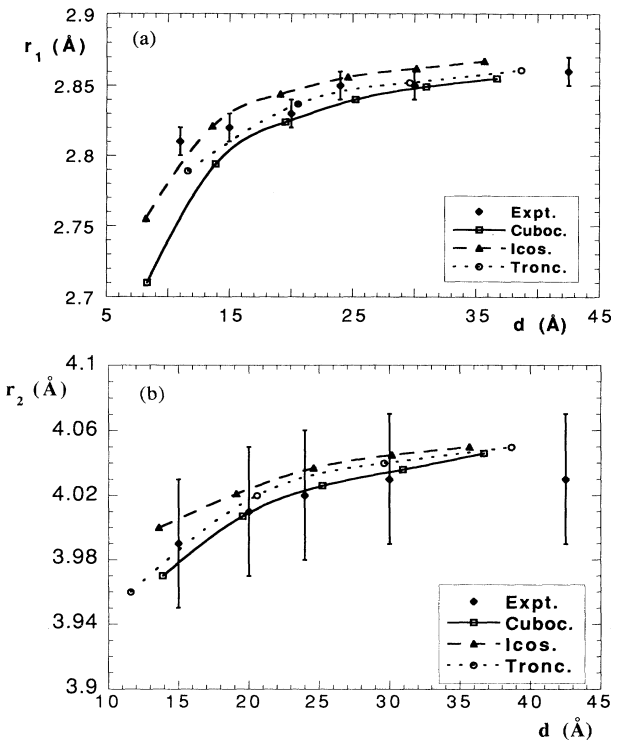

FIG. 2. (a) First neighbors average distance vs clusters size for various structures. The experimental data at $T = 77$ K from Ref. 3 are also reported, labeled by Expt. The labels Cuboc., Icos., and Tronc. refer, respectively, to the cuboctahedral, icosahedral, and troncoctahedral closed-shell structures. (b) Second neighbors average distances vs clusters size for various structures.

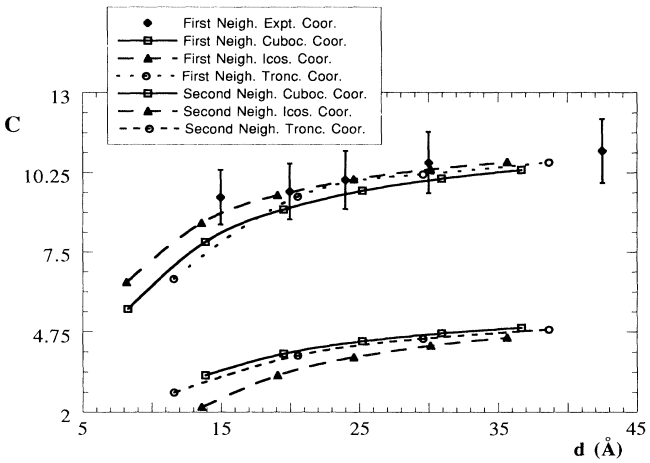

FIG. 3. First and second shell average coordination (C) for various clusters structures compared with experimental values of Ref. 3 at $T = 77$ K. The experimental data obtained by Ref. 3 labeled by Expt. The labels Cuboc., Icos., and Tronc. refer, respectively, to the cuboctahedral, icosahedral, and troncoctahedral closed-shell structures.

shows our data for the quenched structures compared with experimental ones of Ref. 3. The simulation data reported in the picture have been compared by direct integration of radial distributions over the first peak. They perfectly coincide with the theoretical ones relative to the nonquenched structures. This is an indication of the fact that the simulated quenching does not operate any structural transition just relaxing the system. As the experimental data are typically affected by about 10% errors, this graph does not add any further information to the previous ones apart from the datum at $d=15$ Å that suggests a preferred icosahedral structure.

SIMULATED SPECTRA

So far we have been comparing theoretical predictions with the experimental data without taking into account of how these were elaborated. In a sense, implicitly, we assumed a lot of hypotheses on our samples which may or may not be correct. As a matter of fact, it is well known how EXAFS data are strongly influenced by the static and dynamic disorder. When not properly taken into account completely, wrong results may be deduced from the data. To prevent us from such subtle problems we simulated directly the x-rays-absorption spectra.

Once the instantaneous structure of a system is known one can evaluate its contribution to the EXAFS spectra simple applying the well-established formula:[19]

$$\chi^0(k)=\sum_{i=1}^{N}\sum_{j=1}^{N_{(i)}}\chi_{ij}^0(k)\ , \tag{5}$$

where $i\neq j$ and

$$\chi_{ij}^0(k)=\frac{S_0^2 f(k)_j}{kr_{ij}^2}\sin[2kr_{ij}+\phi(k)_{ij}+2\delta(k)_i] \times\exp\left[-2\frac{r_{ij}}{\lambda(k)_{ij}}\right]\ , \tag{6}$$

where k is the photoelectron's wave number, i labels the *central* atom (i.e., the electron emitter atom), j labels the back-scattering atom, f is the back-scattering amplitude, while δ and ϕ are, respectively, the central and back-scattering phase shifts. Although not explicitly written in the formula, the variables f, δ, and ϕ depend also on the distance r_{ij} between the atoms i and j. The exponential factor is the exponential damping term (EDT) that roughly takes into account for the inelastic energy loss of the photoelectron and the finite life of the hole produced by the ionization. The S_0^2 is a many-body amplitude reduction factor due to the multielectron excitations. In principle, this factor depends on the wave vector k and it should be included in any realistic comparison with experimental spectra. In the present paper, we do not intend to compare our simulated EXAFS spectra with experimental ones and hence we assumed $S_0^2=1$. Since developing any suitable model for accounting multiple-electron excitations was far from our purposes, we left the reader the inclusion of a proper factor S_0^2 for direct spectra comparison. A final remark on Eq. (6) concerns the multiple-scattering (MS) contributions to the absorption spectrum. In the present paper we have simulated only single-scattering contributions. Therefore, our simulations lead to reliable results only for first- and second-coordination shells. On the contrary, MS contributions are expected to become significant for the fcc structures when third- and fourth-coordination shells are considered.

In the former picture the cluster structure appears only through the atomic relative distances. Since we have to deal with finite temperature systems, we must develop a formalism for handling thermal vibrations. Coherently with the previous picture this means that we have to average over all the configurations spanned by the system during the time. This is usually taken into account by damping the scattering amplitudes by a Debye-Waller factor:[21]

$$\chi_{ij}(k)=\chi_{ij}^0(k)\exp(-2k^2\sigma_{ij}^2)\ , \tag{7}$$

where σ_{ij}^2 is the mean-square relative displacement (MSRD):

$$\sigma_{ij}^2=\frac{\langle(r_{ij}\cdot\langle r\rangle_{ij})^2\rangle}{\langle r_{ij}\rangle^2}-\langle r_{ij}\rangle^2\ , \tag{8}$$

where the angular brackets $\langle\ \rangle$ indicate the time average and the center dot represents the scalar product.

In the standard EXAFS analysis σ_{ij}^2 are supposed to depend only on the coordination shell regardless of the position of the atoms inside the cluster. It is worth stressing that such a hypothesis does not match the actual situation since atoms on the surface are supposed to oscillate differently from those in the core. For taking into account such different mobility we evaluated separately each σ_{ij}^2, calculating the phonon spectra and eigenvectors of the clusters in the harmonic approximation. In Figs. 4(a) and 4(b) we reported the phonon spectra of the Au_{55} for both the icosahedral and the cuboctahedral structure. The proper frequencies appear to be organized into multiplets of various degenerations. Each element in a multiplet is obtained by acting with the group of symmetry of the cluster over any representative of the multiplet. This means that the quenching did not destroy the clusters symmetries. The cuboctahedral spectrum appears to be spread in a wider frequency interval than the icosahedral ones. Moreover the latter seems to be translated toward higher frequencies. This implies that the icosahedral clusters are more rigid than the cuboctahedral ones. The above consideration is not surprising since it is well known that the icosahedral structure is the most compact. We also evaluated phonon spectra for many other gold clusters. In greater systems frequency degenerations disappeared while the total spectra begin to present the usual Debye shape at low frequencies. Moreover as the size increases the spectra became more spread. Having in mind EXAFS applications we reported in Fig. 5(a) the phonon contribution to the first shell dispersion at $T=20$ K versus the cluster size. As expected, generally speaking the phonon contribution to dispersion decreases with the size and the troncoctahedral points fall along the fcc cuboctahedral interpolation lines. Very small clusters

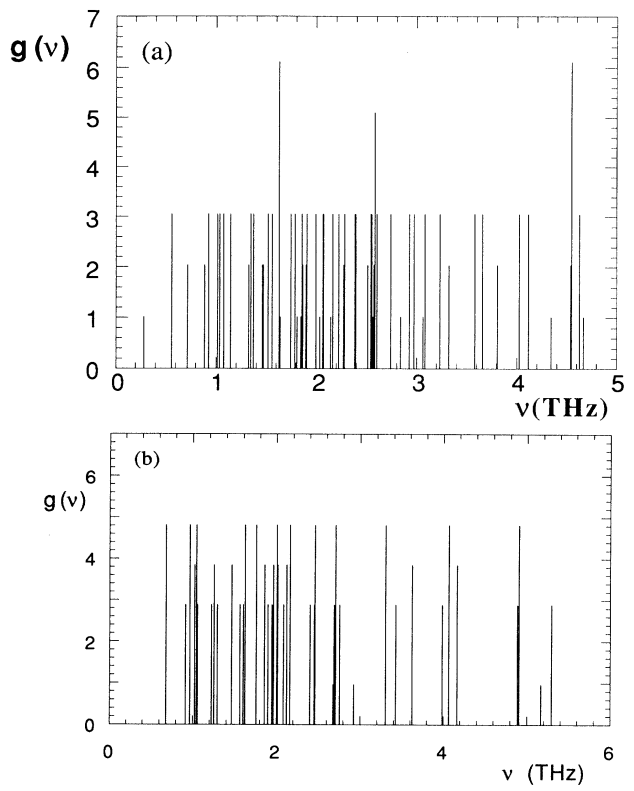

FIG. 4. (a) Phonon spectra of the icosahedral Au_{55}. Ordinates are absolute degenerations of the relative frequences. (b) Phonon spectra of the cuboctahedral Au_{55}.

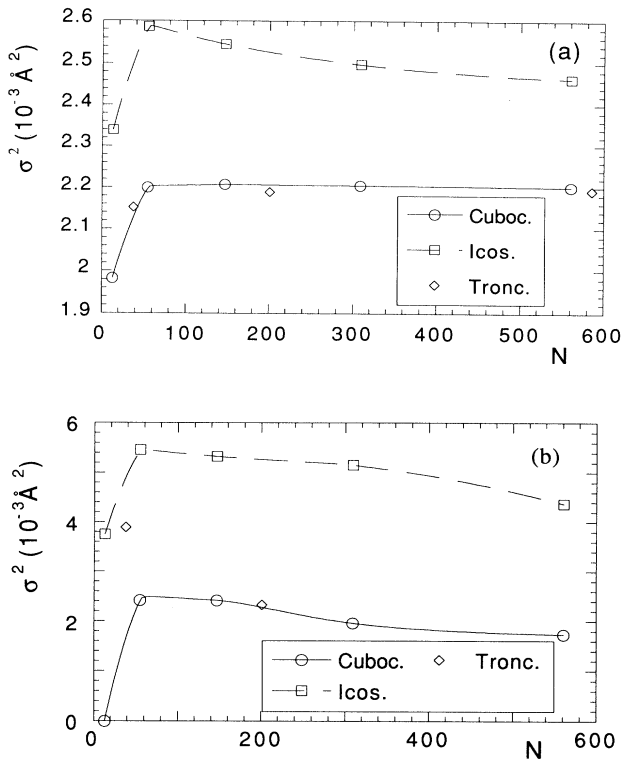

FIG. 5. (a) Phonon contribution to the first shell dispersion. Reported data concern gold clusters of 13, 55, 147, 309, and 561 atoms in both the cuboctahedral and icosahedral structures and of 38, 201, and 586 atoms in the troncoctahedral structure. (b) Static contribution to the first shell dispersion.

($N=13$ and 38) appear to be less sensitive to the temperature than the greater ones. This probably depends on their high degree of compactness. For making comparison we reported in Fig. 5(b) the static contribution to the first shell dispersion of the same clusters. Again, as expected, the contributions tend to decrease with the size. It is worth stressing that the icosahedral static dispersions result to be about twice the correspondent cuboctahedral ones. Moreover cuboctahedral static dispersion tends to vanish with increasing the size while the icosahedral one has an intrinsic component due to the three-dimensional frustration.

Let us now look more carefully at the relative distance fluctuations (σ_{ij}^2). For the sake of concreteness we evaluated the σ_{ij}^2 for each couple i,j of atoms in an Au_{55} cluster at $T=8$ K. As expected the σ_{ij}^2 do not depend only on the relative distance of the atoms i and j but also on their absolute positions inside the cluster. Figure 6 shows all σ_{ij}^2 versus the distance of the first atom from the center of mass. Since every couple appears twice on the graph then, in principle, there could be 2970 different points. Owing to the complete equivalence of all atoms belonging to a fixed radial shell, the number of points drawn reduces drastically. As expected the average MSRD turns out to be an increasing function of the radial distance. As the temperature increases each MSRD increase as well. To illustrate the phenomenon, we reported in Fig. 7 the average MSRD vs temperature for the different shells of an Au_{55} cluster. Again, as expected, the icosahedral structure appears to be generally more rigid than the cuboctahedral one.

Once we get the damping factors we are able to recon-

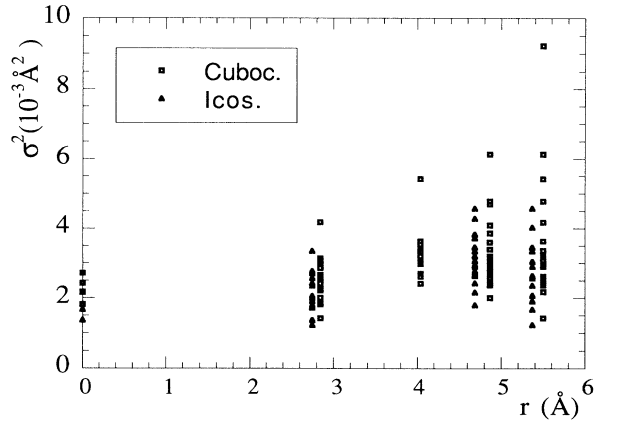

FIG. 6. Au_{55} couples of all σ_{ij}^2 vs the distance of the first atom from the center of mass of the cluster, at $T=28$ K.

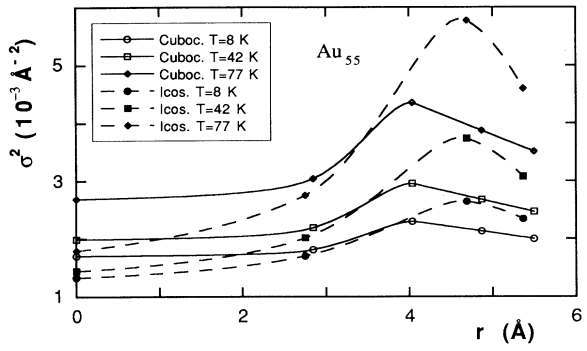

FIG. 7. Au_{55} average σ_{ij}^2 vs temperature for the different shells and structures.

struct the EXAFS signal by means of Eqs. (5), (6), and (7). Equation (6) contains many physical constants described earlier. The amplitude and phase functions we used were obtained by *ab initio* calculations[22] for the photoelectron's scattering in the curved wave formalism, while the empiric values of the λ_{ij} factors have been taken from standard reference data tables.[23] In Fig. 8 we report the resulting spectra at $T=8$ K for both the icosahedral and the cuboctahedral Au_{55} relative to the gold L_{III} absorption edge. The two curves are qualitatively different. The icosahedral one exhibits a greater dominant frequency and a narrower amplitude especially at highest wave vectors K.

Our data on the Au_{55} clusters do not allow one to, unambiguously, assert that the EXAFS spectrum of Marcus *et al.*[1] actually relates to an icosahedral or to a cuboctahedral structure. In fact, all the simulated quantities turn out to be compatible with both structures. The first-neighbor average distance in Marcus experiments is 2.803 ± 0.01 Å, whereas our theoretical calculations give 2.809 Å for the icosahedral geometry and 2.783 Å for the cuboctahedral geometry. In principle this should imply that the involved structure is icosahedral. However, we are not able to *a priori* estimate the level of confidence of our theoretical values. In fact, our potential, which allows very accurate energetic predictions, is very sensitive to changes in the lattice parameter. Such changes could result a scaling of atomic positions thus leading to slightly different results for the first-neighbor average distance. Therefore, looking at the former quantity only, both structures might be compatible with the experimental observation. Similarly, the theoretical coordination numbers (8.5 and 7.85, respectively), which are free of errors, coincide with the experimental value 7.8 ± 1 within the error.

The crucial parameter to discriminate between the structures is the first shell average dispersion, i.e., the variance of the first shell in the radial distribution. This quantity results from the MSRD defined early and from the presence of the "static disorder" that is the component of dispersion due to the static distribution of first-neighbor distances around their average values. We evaluated the global MSRD as the sum of two contributions resulting from the bond vibrations and the static disorder, respectively. All values obtained by such procedure are reported in Tables IV(a) and IV(b) for the icosahedral and the cuboctahedral clusters, respectively. It is worth stressing that the phonon contribution does not disappear as absolute zero is approached. This was expected as a natural consequence of zero-energy vibrations. So far, we have obtained the MSRD just adding its structural and phonon contributions. The first-neighbor dispersion was also obtained by classical MD simulation leading to substantially identical results for temperature of about 100 K. For lower temperatures the dynamic contribution to first-neighbor dispersion tends to zero linearly as expected by classical statistic mechanics.

Let us come back to our comparison with EXAFS experiments, the static value of the MSRD at $T=8$ K for the icosahedral cluster (5.46×10^{-3} Å^2) agrees with the Marcus extrapolated datum (5.7×10^{-3} Å^{-2}). On the contrary, the theoretical value obtained for the cuboctahedral free cluster (2.42×10^{-3} Å^2) is incompatible with the experimental one even assuming at 20% uncertainty in the latter. However, the presence of the ligates

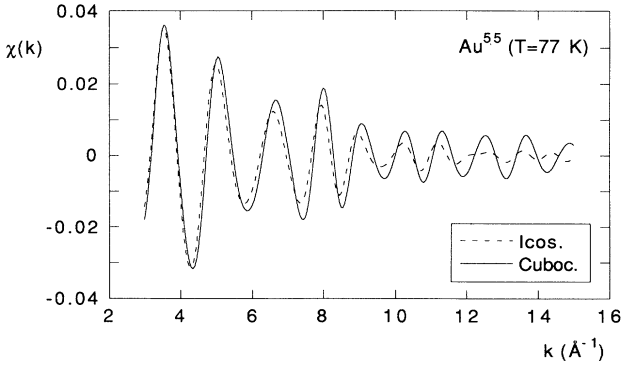

FIG. 8. Simulated Au_{55} EXAFS spectra at $T=8$ K for the two different structures.

TABLE IV. (a) Static and dynamic contributions to the relative mean-square displacements for an Au_{55} icosahedral cluster at various temperatures. (b) Static and dynamic contributions to the relative mean-square displacements for an Au_{55} cuboctahedral cluster at various temperatures.

T (K)	σ^2_{str} (10^{-3} Å^2)	σ^2_{phon} (10^{-3} Å^2)	σ^2_{MSRD} (10^{-3} Å^2)
8	5.46	2.28	7.74
42	5.46	3.05	8.51
77	5.46	4.56	10.02
8	2.42	2.02	4.44
42	2.42	2.50	4.92
77	2.42	3.57	6.00

in Marcus samples may account for the additional amount of static disorder. Therefore the following three possibilities are open.

(i) All clusters in the monodysperse samples of Marcus *et al.* are icosahedral.

(ii) All clusters in the monodysperse samples of Marcus *et al.* are distorted cuboctahedra with a great amount of static disorder due to the presence of ligates (and not to relaxation only).

(iii) The former sample is a mixture of icosahedral and cuboctahedral clusters.

Nevertheless, it is worth stressing that, actually, an icosahedral structure can be seen as 20 distorted fcc pyramids built up along a (1,1,1) direction sharing the vertex in the center of the cluster. So that, owing to the relaxation, the first two interpretations are only slightly different.

Direct spectra comparison are not significant since experimental data refer to clusters enveloped by ligates and thence some slight modification of the atomic positions with respect to the free cluster ones is expected. Moreover our approach to the EXAFS simulation, while taking into account phonon vibration properly, is not one of the most refined.

CONCLUSIONS

Simple tight-binding potential developed first for bulk crystalline gold seems to predict correctly many characteristics of small clusters such as first-neighbor distance contraction and coordination. One of the relevant points emerging from our computation is the critical role played by MSRD in assessing the EXAFS analysis. We overcame this delicate point by directly computing the MSRD via the phonon spectra. It resulted that at least the presence of icosahedral structures is quite necessary to interpret coherently all data in the previous literature. One of the crucial points that may invalidate our conclusion is the comparison with polydisperse samples. We implicitly assumed that clusters with size similar to the closed-shell ones actually present similar structures. It is our opinion that a great deal of effort should be devoted to obtain monodisperse samples. Chemical synthesis is suitable in this respect but does not actually solve the problem since it leads to the presence of surface ligates that may force the clusters in a fixed geometry. In conclusion we suggest direct measures on cluster beams that will provide complete size selection and eliminate any spurious substratum effects.

[1]M. A. Marcus, H. P. Andrews, J. Zegenhagen, A. S. Bommannadar, and P. Montano, Phys. Rev. B **42**, 3312 (1990).
[2]G. Schmid, R. Pfeil, R. Boese, F. Bandermann, S. Meyer, G. H. M. Calis, and J. A. M. Velden, Chem. Ber. **114**, 3634 (1981).
[3]A. Balerna, E. Bernieri, P. Picozzi, A. Reale, S. Santucci, E. Burattini, and S. Mobilio, Phys. Rev. B **31**, 5058 (1985).
[4]P. A. Montano, C. K. Shenoy, E. E. Alp, W. Shulze, and J. Urban, Phys. Rev. Lett. **56**, 2076 (1986).
[5]J. Farges, H. F. De Ferandy, B. Raould, and G. Tochet, J. Chem. Phys. **78**, 5067 (1983).
[6]J. Uppenbrik and D. J. Wales, J. Chem. Phys. **96**, 8520 (1992).
[7]A. L. Mackay, Acta Crystallogr. **15**, 916 (1962).
[8]W. Finnis and J. Sinclair, Philos. Mag. A **50**, 45 (1984).
[9]D. Tomaneck, A. A. Aligia, and C. A. Balseiro, Phys. Rev. B **32**, 5051 (1985).
[10]F. Cleri and V. Rosato, Phys. Rev. B **48**, 22 (1993).
[11]V. Rosato, M. Guillope', and B. Legrand, Philos. Mag. A **59**, 521 (1989).
[12]B. Loisel, D. Gorse, V. Pontikis, and J. Lapujoulade, Surf. Sci. **221**, 363 (1989).
[13]O. B. Christensen, K. W. Jacobsen, and J. K. Norskov, Phys. Rev. Lett. **29**, 2219 (1991).
[14]L. Marville and W. Andreoni, J. Phys. Chem. **91**, 2645 (1987).
[15]F. Ercolessi, W. Andreoni, and E. Tosatti, Phys. Rev. Lett. **66**, 911 (1991).
[16]B. W. van de Waals, J. Chem. Phys. **90**, 3407 (1989).
[17]L. L. Boyer and J. Q. Broughton, Phys. Rev. B **42**, 11 461 (1990).
[18]J. R. Beeler, Jr. and G. L. Kulchinsky, in *Interatomic Potential and Simulations of Lattice Defects,* edited by P. C. Gehlen and J. R. Beeler, Jr. (Plenum, New York, 1971).
[19]P. A. Lee, P. H. Citrin, P. Eisenberger, and B. M. Kincaid, Rev. Mod. Phys. **53**, 769 (1981).
[20]S. Iijame and T. Ichihashi, Phys. Rev. Lett. **56**, 616 (1986).
[21]J. Beni and P. M. Platzman, Phys. Rev. B **14**, 1514 (1976).
[22]A. G. McKale *et al.*, J. Am. Chem. Soc. **110**, 3763 (1988).
[23]M. O. Krause and J. H. Oliver, J. Phys. Chem. Ref. Data **8**, 330 (1979).